

# Mechanics of strength–degrading contact flaws in silicon

B. R. LAWN, D. B. MARSHALL\*, P. CHANTIKUL

*Department of Applied Physics, School of Physics, University of New South Wales, Kensington, NSW 2033, Australia*

The micromechanics of indentation-induced flaws in monocrystalline silicon have been studied in relation to strength determination. In the first part, the evolution of the deformation–fracture pattern during contact with a Vickers pyramid is described. Emphasis is thereby placed on the vital role of the residual component of the elastic–plastic contact field in driving the cracks. In the second part, the response of the cracks in subsequent strength testing is followed. A precursor stage of stable growth is observed prior to attaining a failure configuration, consistent with augmentation of the applied tensile (flexural) loading by the residual contact component. No detectable slow crack growth due to environmental influence is found. Nevertheless, silicon is revealed as a material of extreme susceptibility to brittle fracture, with significant strength degradation from contacts on the microscale. The relevance of this brittleness to the mechanical behaviour of silicon components as a function of fabrication and prospective service conditions is discussed.

## 1. Introduction

The current growth explosion in the semiconductor device industry and in attendant solar cell technology is a commentary on the intense concentration of electronics research on one particular substance – silicon. It is, therefore, somewhat surprising that the mechanical properties of this remarkable material have received little attention in the scientific literature. For, silicon is one of the most brittle of all materials [1], and the incidence of cracking, even on the microscale, can have serious implications in subsequent component performance. Most directly, an incipient microcrack may lead to component malfunction, or even to total failure, if extraneous stresses reach a level at which unstable growth can occur [2, 3]. In a more subtle way, cracks may significantly modify the electronic response, e.g. via the creation of “surface states” at the newly created fracture interface [4, 5].

The question of how microcracks evolve in silicon is thus of some importance if the mechanics

of component degradation are to be understood. In this study a “controlled-flaw” approach, in which a standard Vickers diamond pyramid indenter is used to introduce well-defined deformation–fracture patterns into test surfaces, is adopted. Much attention has recently been devoted to the analysis of these patterns in brittle solids, with the express aim of relating the indentation variables (contact load, characteristic pattern dimensions) to intrinsic material parameters (fracture “toughness”) [6–12]. Apart from providing a convenient means of controlling the scale of microcracking, the indentation method offers considerable physical insight into damage processes associated with fabrication procedures (e.g. scribing with a point tool [3]) or in-service stress-raising events (e.g. particle impact [13]). A key feature in the crack evolution is the vital contribution of residual contact stresses to the net driving force, with consequent deleterious effects in the strength characteristics [10–12]. Strength testing of specimens containing indentation flaws

\*Present address: Materials and Molecular Research Division, Lawrence Berkeley Laboratories, University of California, Berkeley, 94720, USA.

must accordingly reflect on more than just fracture toughness; the material hardness, which quantifies the irreversible component of the contact field, also enters the description. With proper account of the residual stresses one obtains a powerful tool for investigating a wide spectrum of flaw-sensitive mechanical responses in brittle materials; a survey of such responses in the context of evaluating brittle ceramics for structural applications is given elsewhere [14].

In the following sections the indentation–strength behaviour of monocrystalline silicon is examined in detail. The growth history of the induced flaws is considered in terms of two sequentially applied stress fields: (1) the contact field itself, responsible for generating the actual crack system; and (2) a tensile field produced in flexure, responsible ultimately for taking the crack system to failure. The results serve to highlight the extreme susceptibility of silicon to strength-degrading microfracture under normal conditions of component operation.

## 2. Radial crack evolution in elastic–plastic indentation field

The basic elements of the damage pattern produced in Vickers indentation are well established. Around the sharp point of the pyramidal contact the indented material deforms irreversibly, thereby creating a residual hardness impression. In silicon and other solids with the diamond structure the contact stresses are of the order of the theoretical cohesive strength, so a high density of strain energy is available for nucleating microcracks. Although the elements of irreversible deformation have been identified in several transmission electron microscopy (TEM) studies [15–19], the role of these elements in the flaw-generation process remains obscure. The observation of intense diffraction contrast in the regions of material immediately surrounding the indentation sites in the thinned TEM foils [18] attests to the existence of a strong residual component in the “elastic–plastic” stress field. Analogous observations about linear surface scratches made with a diamond scribing tool have been reported by others using X-ray topography [20] and infrared (i.r.) photoelasticity [21].

Above some threshold in the contact loading a well-defined crack system suddenly develops from

the embryo nuclei within the central deformation zone [22]. This threshold is low,  $<0.1N$ , for silicon [23]. Two types of crack form, both in penny-like configuration: (1) “median–radial” cracks [12] (hereafter referred to simply as radial cracks), on the two mutually orthogonal median planes of symmetry defined in each case by the indentation axis and one of the impression diagonals, centred on the contact point (i.e. half-penny cracks); (2) “lateral” cracks, emanating from the base of the deformation zone and spreading laterally outward nearly parallel to the surface. The latter crack type can cause chipping, and is therefore particularly pertinent to the problems of surface wear and erosion; the former type, being more penetrative, bears more strongly on the issue of strength degradation. Since it is the strength behaviour which will be our greater concern here, the radial component will be regarded as the primary crack in the damage pattern.

Silicon is, of course, opaque to light in the visible region of the spectrum, so direct observation of subsurface crack development during the contact cycle is not feasible. A fractographic technique involving examination of the crack surfaces after the event was accordingly used [10]. The specimens were single-crystal slices 1 mm thick with an optical quality surface finish. Although the indentation axis was aligned accurately along the near- $\{111\}$  surface normal, no attempt was ultimately made to orientate the impression diagonals along a specific crystallographic direction; preliminary tests showed experimental scatter to mask any systematic anisotropy in the crack pattern.\* After indentation in air, each specimen was broken by applying a tensile stress normal to one of the median planes (in three-point bending, as described in Section 3), thereby affording a cross-sectional view of the entire subsurface radial crack system. An example is shown in Fig. 1, with a schematic diagram to illustrate how the observed fracture markings (due mainly to spurious disturbances in the indenter drive) relate to the overall damage pattern. The markings reveal a growth history similar to that previously described for glass [10, 12]: during the loading half-cycle the crack is driven outward, but is constrained somewhat at the surface by a compressive component in the elastic point-

\*Diamond-type crystals have a  $\{111\}$  cleavage tendency, but this tendency is not strong: on a simplistic bond-count basis a maximum variation of  $3^{1/2}$  is estimated in the surface energies in going from  $\{111\}$  to  $\{110\}$  planes [24].

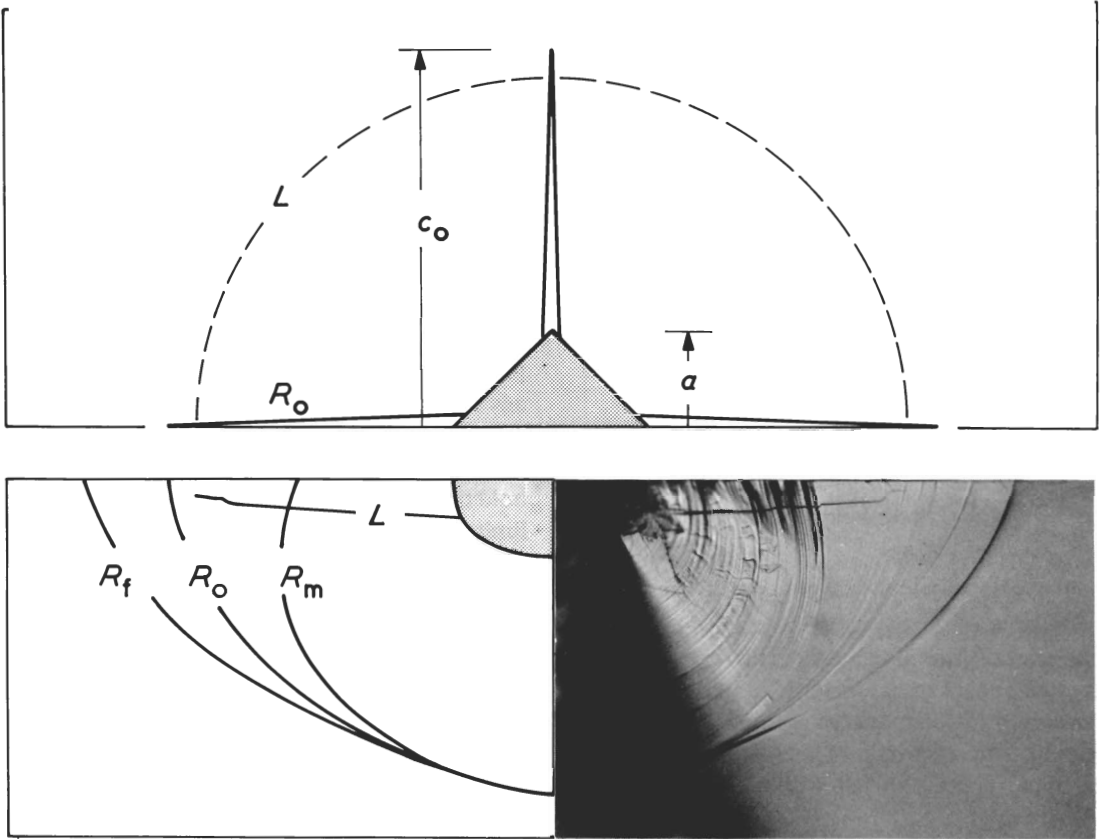


Figure 1 Radial–median crack system in silicon. Micrograph is half-view of crack formed at  $P = 30$  N, photographed after fracture on median plane. Schematic diagram at left bottom depicts essential features of fractographic pattern: radial crack front at maximum contact load ( $R_m$ ), at complete unload ( $R_o$ ), and at failure in subsequent tensile stressing ( $R_f$ ); trace of lateral crack ( $L$ ); deformation zone (shaded). Schematic diagram at the top depicts surface view at complete unload, indicating characteristic dimensions of radial cracks ( $c_0 = 170 \mu\text{m}$ ) and deformation impression ( $a = 41 \mu\text{m}$ ).

contact field; during unloading the elastic constraint relaxes, and the radial crack trace continues to extend under the sustained action of the residual stresses generated by elastic–plastic mismatch. In direct contrast to the glass observations, however, the radial cracks showed no tendency to further growth *after* removal of the indenter, suggesting that silicon is not susceptible to atmosphere-enhanced slow crack growth. Surface chipping was also more prevalent in silicon, particularly at higher contact loads, often severely disrupting the surface radial pattern.

Thus the radial crack experiences a persisting driving force which, expressed as a residual stress intensity factor, takes the form [10]

$$K_r = \chi_r P / c_0^{3/2} \quad (1)$$

where  $P$  is the peak contact load,  $c_0$  is the crack length at completion of the contact (Fig. 1), and  $\chi_r$  is an elastic–plastic constant. Since the surface

crack grows stably up to the point of final withdrawal of the indenter, the equilibrium condition  $K_r = K_c$  must apply, where  $K_c$  defines the material toughness. Hence from Equation 1

$$P / c_0^{3/2} = K_c / \chi_r = \text{constant}. \quad (2)$$

Fig. 2 shows results obtained from the indentation tests on silicon (the value of  $c_0$  for each indentation being averaged over the four radial traces); the mean and standard deviation over all indentations gives  $K_c / \chi_r = 12.5 \pm 1.8 \text{ MPa m}^{1/2}$ . A detailed analysis of the elastic–plastic parameter in Equation 1 yields the relation  $\chi_r = 0.014(E/H)^{1/2}$ , where  $E$  and  $H$  are the Young's modulus and hardness (here defined as  $P/2a^2$  for the Vickers geometry in Fig. 1), and the numerical constant is obtained by calibration with glass as a standard material (random error  $< 10\%$ ) [12]. Thus for silicon, taking  $E = 168 \text{ GPa}$  [25] and  $H = 9.0 \text{ GPa}$ ;  $K_c = 0.76 \pm 0.19 \text{ MPa m}^{1/2}$  is obtained as an

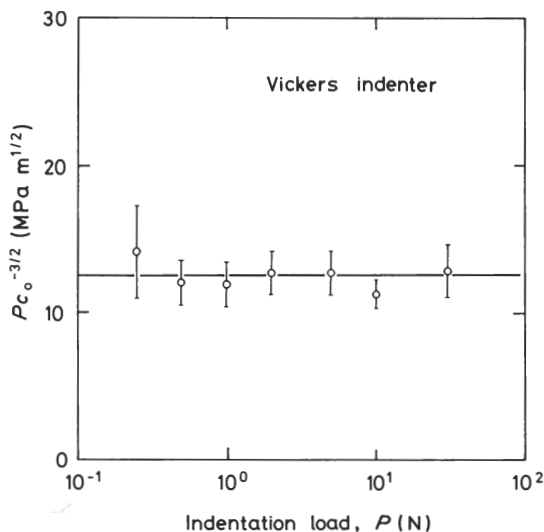


Figure 2 Plot of  $P/c_0^{3/2}$  against  $P$  for silicon. Each data point is the mean and standard deviation of 7 indentations.

estimate of the toughness. This compares with fracture mechanics determinations by other workers [25–28], whose quoted values, corresponding to a variety of techniques and crystallographic planes, all fall within the range  $0.5$  to  $1.0 \text{ MPa m}^{1/2}$ .

### 3. Mechanics of failure from the radial crack system

Now the response of the radial crack system to a post-indentation tensile stress is considered. Detailed observations in glass [11] show that the applied tensile field is augmented by the residual field in such a way that the crack undergoes a precursor stage of stable expansion prior to reaching a failure configuration. The corresponding failure stress is significantly less (typically by  $\approx 30$  to  $40\%$ ) than would be expected from the conventional theory of strength. It is of considerable interest to investigate whether this effect extends to silicon; for, if it does, any contact-induced flaw becomes a more likely source of premature breakdown in a component.

For this purpose a series of strength tests was run on sample bars cut from the (111) silicon slices; again, no attempt was made to orient the bars in any specific crystallographic direction along their length or width. Each bar (measuring  $25 \text{ mm} \times 3 \text{ mm} \times 1 \text{ mm}$ ) was indented at the centre of a major face, at a load of  $P = 30 \text{ N}$ , with the radial cracks aligned parallel to the edges. A simple cylindrical-support arrangement was contrived to

stress the bars in three-point bending (span  $10 \text{ mm}$ ), with the indentation site in the region of maximum tension. The bending force was delivered via a motor-driven double screw, and was simultaneously monitored by an instrumented proving ring [29]; simple-beam theory was then used to evaluate the corresponding bending stress. The entire stressing system was mounted onto the stage of an inverted microscope, so that the progress of the critical radial crack could be followed *in situ*. All testing was carried out in air. As with the preceding indentation observations, no evidence of any chemically-enhanced slow crack growth was found: e.g. bars loaded to within  $99\%$  of the failure stress showed no detectable extension over  $5 \text{ min}$  hold time (which, in conjunction with an estimated limit of  $\approx 5 \mu\text{m}$  in resolution of the crack-tip position, corresponds to a velocity of  $\leq 10^{-8} \text{ m sec}^{-1}$  at  $K = 0.99K_c$ ).

The radial crack growth to failure is plotted in Fig. 3 as applied tensile stress  $\sigma_a$  against crack size  $c$  (averaged over the two radial traces which constitute the critical crack, i.e. that crack perpendicular to the stress axis), for four bend specimens. In each case the existence of a precursor stage of extension is apparent, demonstrating the influence of the residual field. However, this extension does

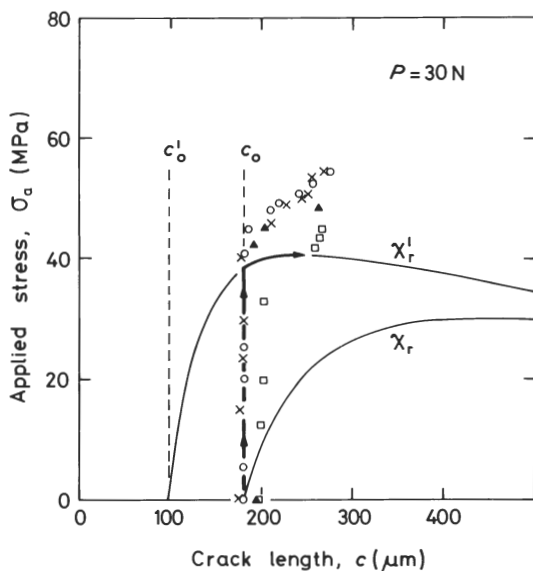


Figure 3 Radial crack growth in bend tests on pre-indented silicon bars (each symbol represents an individual bar). Curves are plots of Equation 4 corresponding to unrelaxed ( $\chi_r$ ) and relaxed ( $\chi_r'$ ) residual fields, with arrowed lines designating the appropriate crack path to failure.